Global change and climate-driven invasion of the Pacific oyster (Crassostrea gigas) along European coasts: a bioenergetics modelling approach

Yoann Thomas, Stéphane Pouvreau, Marianne Alunno-Bruscia, Laurent Barillé, Francis Gohin, Philippe Bryère, Pierre Gernez

Journal of Biogeography
March 2016, Volume 43, Issue 3, Pages 568-579
http://dx.doi.org/10.1111/jbi.12665
http://archimer.ifremer.fr/doc/00287/39828/

Global change and climate-driven invasion of the Pacific oyster (*Crassostrea gigas*) along European coasts: a bioenergetics modelling approach

Thomas Yoann [1, *], Pouvreau Stephane [2], Alunno-Bruscia Marianne [2], Barillé Laurent [1], Gohin Francis [3], Bryère Philippe [4], Gernez Pierre [1]

[1] Mer Molécules Santé EA 2160; Faculté des Sciences et des Techniques; Université de Nantes; Nantes cedex 3 44322 France
[2] UMR 6539; Ifremer; Argenton-en-Landunvez 29840 France
[3] DYNECO/PELAGOS; Ifremer; Plouzané 29280 France
[4] ACRI-HE; Brest 29200 France

* Corresponding author : Yoann Thomas, email address : yoann.thomas1@gmail.com

Abstract :

Aim

The spread of non-indigenous species in marine ecosystems world-wide is one of today's most serious environmental concerns. Using mechanistic modelling, we investigated how global change relates to the invasion of European coasts by a non-native marine invertebrate, the Pacific oyster *Crassostrea gigas*.

Location

Bourgneuf Bay on the French Atlantic coast was considered as the northern boundary of *C. gigas* expansion at the time of its introduction to Europe in the 1970s. From this latitudinal reference, variations in the spatial distribution of the *C. gigas* reproductive niche were analysed along the north-western European coast from Gibraltar to Norway.

Methods

The effects of environmental variations on *C. gigas* physiology and phenology were studied using a bioenergetics model based on Dynamic Energy Budget theory. The model was forced with environmental time series including *in situ* phytoplankton data, and satellite data of sea surface temperature and suspended particulate matter concentration.

Results

Simulation outputs were successfully validated against *in situ* oyster growth data. In Bourgneuf Bay, the rise in seawater temperature and phytoplankton concentration has increased *C. gigas* reproductive effort and led to precocious spawning periods since the 1960s. At the European scale, seawater temperature increase caused a drastic northward shift (1400 km within 30 years) in the *C. gigas* reproductive niche and optimal thermal conditions for early life stage development.

Main conclusions

We demonstrated that the poleward expansion of the invasive species *C. gigas* is related to global warming and increase in phytoplankton abundance. The combination of mechanistic bioenergetics modelling with *in situ* and satellite environmental data is a valuable framework for ecosystem studies. It offers a generic approach to analyse historical geographical shifts and to predict the biogeographical changes expected to occur in a climate-changing world.

Keywords : biogeographical range expansion, *Crassostrea gigas*, DEB model, European coasts, functional traits, global change, individual-based model, invasive species, remote-sensing

1. INTRODUCTION

In coastal ecosystems, global change affects marine communities by inducing variation in abundance and geographic shifts (Helmuth *et al.*, 2006b; Beaugrand *et al.*, 2009; Saupe *et al.*, 2014). Beyond processes such as predation, dispersal or habitat availability, modification of species-specific physiology and phenology are direct effects of climate change at the organism level, with subsequent consequences for populations and ecosystems (Pörtner *et al.*, 2001). Changes in metabolic rates and life-cycle timing affect organism and population growth rates, as well as species interactions. In order to develop a comprehensive and predictive ecosystem approach, it is essential to understand the processes underpinning the response of coastal communities to global change (Teal *et al.*, 2012; Sarà *et al.*, 2013).

Concurrently to modifications in the natural range distributions of indigenous species, the spread of non-indigenous species appears to be facilitated by global change (Stachowicz *et al.*, 2002). Environmental changes such as seawater warming and coastal eutrophication can allow reproduction, larval survival, and recruitment of marine benthic species beyond their present distribution range (Diederich *et al.*, 2005). In receiving ecosystems, consequences of biological invasions are readily identifiable when invasive species are ecosystem engineers such as polychaetes or bivalves. These organisms modify habitat structure, change hydro

sedimentary processes through filtration, ingestion and biodeposition of suspended particles and impact spatial and/or trophic competition, ultimately leading to modifications in the biodiversity of local biota (Briggs, 2007; Troost, 2010).

The Pacific oyster, *Crassostrea gigas* (Thunberg, 1793), was introduced to the Atlantic European coasts at the end of the 19th century for shellfish culture purposes (Humphreys *et al*., 2014) and is the main oyster species farmed in Europe today. During recent decades, the Pacific oyster acquired invasive species status with the expansion of its biogeographic distribution along the northwestern European coasts beyond the area of its initial introduction to farming sites. The expansion of wild settlement in Europe can be observed through the formation of dense reefs, which drastically change the physical characteristics of both soft and hard substrates (Lejart & Hily, 2011). Several field studies have reported a correlation between this expansion and the increase in seawater temperature, mainly since 1995, related to better reproduction, larval development and recruitment rates (Diederich *et al*., 2005; Schmidt *et al*., 2008; Dutertre *et al*., 2010). The increase in water temperature expected in the 21st century (IPCC, 2007) may exacerbate the expansion of *C. gigas* along NW European coasts and, on a greater scale, along the latitudinal range of its current worldwide biogeographic distribution (Carrasco & Barón, 2010), but multiple vectors of transport between water bodies (e.g. ballast water, fouling and the transportation of spat for aquaculture) are also to be considered. While empirical relationships between population dynamics and environmental variables provide a basis for assessing environmental responses, a mechanistic approach, accounting for functional interactions, is needed to elucidate and quantify the processes underlying ecosystem response to global change (Teal *et al.*, 2012; Kristiansen *et al.*, 2014). Mechanistic models are valuable tools for this purpose, and modelling approaches are useful for gaining a quantitative understanding of the effects of

environmental changes on marine communities, and predicting their responses to projected climatic trends.

In the present study, we investigated the long-term changes and large-scale variations in the Pacific oyster's life history traits over the last 50 years. We analysed the effects of environmental variability on the growth and reproduction of the species, and estimated the consequences of environmental changes on its geographic range along the NW European coasts. To this end, a Dynamic Energy Budget (DEB) model was implemented to explore the historical growth and reproductive patterns of *C. gigas*. The DEB model offers a generic framework to describe the energy flow through an organism in a varying environment (van der Meer, 2006; Kooijman, 2010). It covers the full life cycle of an individual and provides quantitative information on mass and energy balances. Several applications of the DEB model demonstrated its ability to mechanistically examine bivalve physiological responses to environmental changes and quantify the consequences in terms of growth, physiological condition and reproductive output (Bernard *et al*., 2011; Sarà *et al*., 2013).

The paper is organized into three parts: model calibration, model application, and a large-scale retrospective analysis. The first part examines the ability of the model to simulate seasonal and inter-annual variations in growth and reproductive patterns of *C. gigas* observed at a study site (Bourgneuf Bay). The model is then applied to investigate the long-term reproductive traits of the Pacific oyster in Bourgneuf Bay over the last 50 years, allowing us to analyse the temporal variations of life history traits important for the geographical expansion of the species (oocyte production, spawning dates). The last part broadens the geographical perspective by using satellite data to analyse the large-scale expansion of *C. gigas* reproductive niche along European Atlantic coasts in the context of global warming.

MATERIALS AND METHODS

Study site

Long considered as the northern boundary of Pacific oyster distribution in western Europe (Goulletquer & Héral, 1991), Bourgneuf Bay is a 340-km^2 embayment located south of the Loire estuary on the French Atlantic coast (2°W, 47°N, Fig. 1). This turbid bay is connected to the ocean by a 12 km opening in the northwest, and to the south by a channel 800 m in width. Intertidal areas cover 100 km^2 of its area. Extensive aquaculture of *C. gigas* has been conducted in Bourgneuf Bay since the 1950s. Oysters are farmed over 1000 ha of the intertidal zone, with yearly production ranging from 8600 to 10 000 tonnes in the last decade and a stock of around 45 000 tons (Fig. 1). Concurrently, a large wild stock has colonized natural rocky areas and oyster-farming sites (Cognie *et al.*, 2006).

The oyster-DEB model

The oyster-DEB model was derived from the standard DEB model described by Kooijman (2010) and first applied to *C. gigas* by Pouvreau *et al.* (2006). The model equations and parameter values used here are based mainly on the study performed by Bernard *et al.* (2011), which refined the processes of energy allocation to gametogenesis and resorption. The conceptual scheme of the model is described in Fig. S1 in Appendix S1 in Supporting Information. Further details on DEB model principles and initialization are described in Appendix S1. The flux equations and parameters are summarized in Tables S1 and S2, respectively. To assess the reproductive effort, individual oocyte production was estimated from the cumulated energy allocated to the gamete buffer with the cost of production of a single oocyte of 9.3×10^{-4} J. In the oyster-DEB model, spawning is triggered when two thresholds are reached: a seawater temperature threshold set at 18°C and a gameto-somatic

index (GSI) threshold of 40%, where GSI is defined as a mass ratio between the gonadic and total dry flesh mass (Pouvreau *et al.*, 2006).

Individual-based simulations

To account for inter-individual variability, the DEB model was applied through an individual-based modelling (IBM) strategy. Individual growth simulations were then pooled together to compute average growth patterns and inter-individual standard deviation. Inter-individual variability was introduced into the DEB model though: (1) an individual initial state computed according to the initial oyster length (L) and dry flesh mass (DFM), and (2) a specific model parameterization of the ingestion function for each individual. Indeed, faster growth is usually associated with faster rates of feeding (Tamayo *et al*., 2014). Therefore, following Bacher & Gangnery (2006), inter-individual variability in growth potential was assumed to be related to the half-saturation coefficient of the functional response, X_K (Eq. 2' and 2'', Table S1). X_K values were allocated to each individual following a Gaussian distribution with an average of 0.32×10^6 cell L^{-1} (Table S2) and a standard deviation of 0.06×10^6 cell L^{-1} in order to associate the smallest X_K with the fastest-growing oyster and vice versa.

Forcing variables

The standard DEB model takes into account two forcing variables: food concentration and seawater temperature. When exposed to high concentrations of particulate inorganic matter (PIM), oysters can develop physiological adaptations to maximize organic ingestion through pseudo-faeces production. We therefore introduced PIM concentration as a third forcing variable, related to the ingestion function following Kooijman's conceptualization (2006) (see equations 2' and 2'' in Table S1).

Phytoplankton concentration was used as the food source. Species identification and cell number from March 1998 to December 2013 were extracted from the national REPHY network for phytoplankton monitoring. Sampling was performed monthly at the station “Bois de la Chaise” in Bourgneuf Bay (Fig. 1). It had already been shown that two bloom-forming species, *Leptocylindrus sp.* and *Lepidodinium sp.* did not contribute to oyster growth, presumably due to very low assimilation efficiency (Bourlès *et al.*, 2009; Alunno-Bruscia *et al.*, 2011). These two species were then excluded from the total phytoplankton counts. A summary of the forcing variable values is given in Appendix S2 and Figure S3 in Supporting Information.

The two other forcing variables, namely PIM concentration and sea surface temperature (SST), were obtained using satellite observations. Daily PIM concentration was obtained using merged SeaWiFS, MODIS and MERIS data, as described in Saulquin *et al.*, (2011) using a regional algorithm specifically designed for the coastal waters of the Bay of Biscay (Gohin, 2011). PIM concentration maps were extracted over Bourgneuf Bay for the period 1998–2013. Daily SST data were obtained from the Advanced Very High Resolution Radiometer (AVHRR) for the period 1986–2009 (Saulquin & Gohin, 2010), and from the Group for High Resolution Sea Surface Temperature (GHRSST) initiative for the second period 2010–2013 (Dash *et al.*, 2012). For this second period, OSTIA/MetOffice and ODYSSEA/Ifremer interpolated SST products were provided by Copernicus/MyOcean.

Model validation

The predicted DFM growth patterns and reproductive traits were compared to a 16-year time-series data set (1998 to 2013). *In situ* L and DFM measurement were performed as part of the national monitoring program on oyster growth and survival (REMORA and RESCO networks; http://wwz.ifremer.fr/observatoire_conchylicole). A set of 300 18-month-old

oysters naturally recruited and grown in Arcachon Bay (France) was deployed every year from March to December in Bourgneuf Bay in the oyster-farming sector of “La Coupelasse” (Fig. 1). Individual L and DFM were measured on a subset of 30 individuals, every 3 months from 1998 to 2008, and at bi-weekly or monthly scale from 2009 to 2013.

Individual-based DEB simulations of 30 individuals were performed each year, from March to December, on the 16-year period 1998–2013, as described in Appendix S1. The goodness of fit between observed and predicted DFM was tested following individual profiles, giving an estimation of the growth pattern, including reproductive traits, and inter-individual variance accuracy.

Model application

Oyster ecophysiological responses to environmental changes were studied with another set of DEB simulations, performed each year using the same pool of standard individuals to avoid variability associated with the yearly initial state of the oysters monitored. An IBM approach was computed, using initial L and DFM of every individual (n = 480) within the 16-year dataset of measured initial biometrics. Simulations were performed yearly (i.e. from 1 March to 15 December) from 1998 to 2013 using observed SST, phytoplankton and PIM concentration. Relationships between life history traits (i.e. maximum DFM, oocyte production and spawning date), and environmental variables (food and temperature) were examined.

Large-scale retrospective simulations

First, the long-term consequences of global warming on spawning traits of *C. gigas* were evaluated in Bourgneuf Bay. Yearly growth was simulated with the IBM-DEB model from 1960 to 2013 using daily SST, phytoplankton and PIM concentration data. Since no SST

measurements were available for Bourgneuf Bay before 1998, the seawater temperature was reconstructed from 1960 to 1998 using daily air temperature data collected in Bourgneuf Bay (source: Météo-France). No data on phytoplankton or PIM concentrations were available before 1998 in Bourgneuf Bay. To estimate the sensitivity of oyster's reproductive niche to the trends in plankton and PIM in parallel with the SST patterns, three scenarios were tested consisting of low, mean and high phytoplankton and PIM concentrations (see Appendix S2, Fig. S4). Daily values of phytoplankton and PIM were used in order to maintain their seasonal patterns. The yearly spawning dates were then extracted from the DEB simulations. These results were analysed in relation to summer SST conditions, in order to relate the timing of larval appearance to the environmental conditions that the oysters would experience during their early stage of life.

Second, pan-European satellite-derived SST data was used to investigate the large-scale spatial patterns of reproductive traits and thermal conditions along the NW European coasts since 1986. The DEB model simulations were spatialized and yearly simulations were performed for every satellite pixel, using daily SST satellite observations, according to the three food scenarios previously described (low, mean and high phytoplankton and PIM concentrations). Yearly spawning dates were extracted from the simulations performed for every satellite pixel. The combination of satellite data with DEB simulation was used to map *C. gigas* spawning dates along the NW European coast from 1986 to 2013, from Gibraltar to Norway.

Statistical analysis

The agreement between field observations and model simulations was quantified using a Taylor diagram. A Taylor diagram provides a statistical summary of how predictions match observations in terms of correlation, root-mean-square (RMS) difference and variance ratio

(Taylor, 2001). Linear regression and Pearson correlation were used to test the trend in predicted life history traits as well as their relations with environmental forcing. Analysis of variance (ANOVA) was used to test the null hypothesis of no difference in spawning date and summer SST according to the time factor and to the three food and PIM scenarios. All statistics were performed using R v3.1.1 software (R Development Core Team, 2012).

RESULTS

Model validation

The simulated DFM trajectories coincided with observations over the entire 16-year period. Most years showed a good fit between observations and simulations, with a correlation coefficient up to 0.8 and a normalized standard deviation close to 1 (Fig. 2). Two types of spawning events can be observed from individual trajectories: synchronous events, with all individual spawns occurring at the same time (years 1998–2000, 2002, 2006, 2007, and 2009–2012); and asynchronous events, showing one or two spawns of lower intensity at intervals of several weeks (years 2003–2005, 2008, and 2013) (e.g. Fig. 3a–d for 2004, 2008, 2009 and 2012; and Fig. S2 for all years). The most asynchronous year was 2008, with spawning events occurring from June to September; this was well accounted for by the unusual standard deviation observed in the DFM data in mid-July (Fig. 3b).

Model application

The oyster growth time series showed strong inter-annual variability in spring for all years, with the highest values observed in 2012 and 2013 (Fig. 3e). During summer, a decrease in the tissue mass made it possible to pinpoint spawning events. Maximum DFM increased significantly between 1998 and 2013 (Fig. 4a, linear regression: $r^2 = 0.32$, $P = 0.014$, slope =

0.067 g year^{-1}). Maximum DFM was reached in 2013, at 3.05 ± 0.67 g, and the minimum occurred in 2001, at 0.97 ± 0.19 g. Oocyte production similarly showed a significant increase between 1998 and 2013 (Fig. 4b, linear regression: $r^2 = 0.51$, $P = 0.001$, slope = 2.2×10^6 oocyte year^{-1}), varying from 25.5×10^6 to 76.1×10^6 oocytes, respectively. Concurrently, no significant trend was observed in spawning date during the same 16-year period (Fig. 4c, linear regression: $P = 0.73$).

Three significant relations were observed between the late-spring environmental conditions (averaged from 1 June to 15 July) and the life history traits of the Pacific oyster. The maximum DFM and cumulated oocyte production were positively correlated with the late-spring phytoplankton concentration (Fig. 5a–b, linear regression: $r^2 = 0.61$ and 0.49, $P < 0.001$ and $P = 0.002$, slope = 0.45 g ($\times 10^6$ cell L^{-1})$^{-1}$ and 1.09×10^7 oocytes ($\times 10^6$ cell L^{-1})$^{-1}$, respectively). The spawning date was inversely related to the late-spring SST (Fig. 5c, linear regression: $r^2 = 0.74$, $P < 0.001$ and slope = -24 day °C^{-1}). High late-spring SST led to earlier spawning dates, which occurred as early as mid-June, e.g. in 2003. Late spawning events were associated with lower late-spring SST, e.g. in 2002, when spawning occurred as late as 19 August. Neither maximum flesh volume, nor cumulated reproductive effort had a significant relationship with spawning time or any of the forcing variables.

Large-scale retrospective simulations

A significant increase in yearly-averaged SST was observed during the last 50 years in Bourgneuf Bay, (Fig. 6a, linear regression: $r^2 = 0.32$, $P < 0.001$ and slope = 0.015 °C year^{-1}). The projection of summer SST on spawning dates supports the idea that a shift occurred in the last century (Fig. 6b). Most years from 1960 to 1987 were associated with late spawning events and cooler summer conditions, while precocious spawning events and warm summers characterized most years from 1988 to 2013. A significant phenological shift of 8 days in the

spawning date and a difference of 0.4°C in summer SST were found between these two groups (ANOVA, Table 1). No significant difference was found between the three investigated food and PIM scenarios (ANOVA, Table 1).

The simulated spatial distribution of *C. gigas* spawning date along the NW European coast was compared between the two most contrasted cold and warm years: 1986 (annual mean SST for Europe: 12.99°C) and 2003 (annual mean SST for Europe: 14.25°C) (ANOVA, d.f. = 1, $F = 18.9$, $P < 0.001$) (Fig. 7). A south-north gradient is clearly shown in both 1986 and 2003, with spawning events occurring earlier in the south of Europe. In 1986, the main boundary of the temporal spawning window was located close to the Loire estuary (47.2°N), although a number of isolated spawning events were also likely to occur in several embayments located further north, up to 55°N, scattered from the Belgian to south-western Danish coasts in the North Sea and Kattegat Bay. The 2003 map showed a drastic shift of the northern boundary, and the possibility of spawning events occurring as far north as the southern Norwegian coast (60°N). However, some areas, e.g. northwestern Brittany, showed no spawning events, even in these warm conditions. Only marginal differences were found between the three investigated food and PIM scenarios. These differences occurred close to the Danish coasts, with a spawning area restricted by low food and PIM, and in Mediterranean waters, with an earlier start of the spawning window with high food and PIM levels.

A similar shift northward was observed in the summer SST (Fig. 8). The SST boundary of 18°C, which was located close to the Charentais sounds (46°N) in 1986, had moved northward to the western Danish coasts (56°N) by 2003. The western Baltic Sea and Swedish coasts (up to 56°N) also presented favourable thermal conditions the same year.

DISCUSSION

The biogeographic expansion range of many intertidal species shifted poleward by as much as 50 km per decade during the last century (Helmuth *et al*., 2006b). In particular, the non-native species *C. gigas* showed invasive behaviour on European Atlantic coasts, and extended its geographic range from the south of France to Norway over the last 50 years. The increasing reproductive success that accompanied this expansion led to the formation of wild oyster reefs on many rocky and soft substrates. In this context of global change and biological invasions, we developed a mechanistic approach to understanding and predicting physiological and phenological responses of *C. gigas* to large-scale and long-term environmental variability. Our approach went beyond correlated relations and made projections on a spatially explicit scale.

The Dynamic Energy Budget (DEB) theory provides a framework for generic and mechanistic modelling that is suitable for exploring species phenotypic traits and spatio-temporal distributions (Kearney et al., 2010). In addition, individual-based modelling (IBM) has now been recognized as a valuable approach in ecology and evolutionary biology, including bioenergetics modelling of life history traits (DeAngelis & Mooij, 2005). The present work was built upon recent developments of the oyster-DEB model (Pouvreau *et al.*, 2006; Bourlès *et al.*, 2009; Alunno-Bruscia *et al.*, 2011; Bernard *et al.*, 2011). These improvements include the use of selected phytoplankton communities as forcing, the addition of the influence of PIM concentration on the ingestion and improvement of the gametogenesis processes. The upgraded IBM-DEB approach led to a satisfactory agreement between simulations and actual observations of growth and reproductive traits over a 16-year period. The IBM improved our understanding of the bioenergetics contribution to spawning synchronicity, which is recognized as one of the main factors determining reproductive success (O'Connor *et al*., 2007). IBM simulations showed that synchronous spawns were

mainly triggered by temperatures exceeding the SST threshold of 18°C when individuals had already reached the gameto-somatic index (GSI) threshold. In contrast, asynchronous events occurring once SST exceeded 18°C were dependent on the GSI threshold. The occurrence of synchronous and asynchronous spawns did not depend on oysters' initial state, but on their individual response to environmental changes. This demonstrates that the environmental variability experienced by juveniles affect the bioenergetics balance at individual scale, and subsequently leads to phenological changes at the scale of a population, as already observed by Enriquez-Diaz *et al.* (2009).

A significant increase in maximum dry flesh mass and oocyte production was evident in the simulated time-series. From 1998 to 2013, the production of gamete was estimated to increase from 20 to 70 $\times$ 10^6 oocytes per oyster. This increase by a factor of 3 coincides with experimental observations (Chavez-Villalba *et al.*, 2003). A positive relationship between phytoplankton abundance and oyster growth (in terms of maximum DFM and reproductive effort) was observed in Bourgneuf Bay over the last 16 years, suggesting that oysters were generally food-limited. More precisely, the decadal change in fitness potential was related to a late-spring increase in phytoplankton concentration. The reasons for the increase in phytoplankton abundance over the last decades remain to be elucidated. Climate change, and more precisely global warming, is generally considered to cause trophic amplifications (Kirby & Beaugrand, 2009) and significant shifts in phytoplankton phenology, abundance and composition (Hernández-Fariñas *et al.*, 2013). The resulting effect on oyster ecophysiology is however not straightforward, as some phytoplankton are not suitable for ingestion by bivalves (Beninger *et al*., 2008). In our simulations, the selection of ad-hoc phytoplankton species allowed a better quantification of *C. gigas* growth patterns. The DEB theory may prove useful to investigate the food preferences of filter feeders such as *C. gigas* (this study) or *Mytilus edulis* (Picoche et al., 2014). Further work is needed to better characterize the actual food

consumption and selective feeding behaviour of a variety of bivalve species, and to more realistically model the functioning of shellfish ecosystems.

A significant shift in oyster phenology was demonstrated, indicating precocious spawning events since the end of the 1980s. Concurrently, thermal conditions of the early oyster life stages became more favourable, supporting optimal development conditions that shorten the duration of the pelagic larval stage and increase the larval supply since this time period. Dependent on the global rise in SST, the spread of *C. gigas* has been reported in several coastal ecosystems, from European to New Zealand coasts (Diederich *et al.*, 2005). Our study seeks to improve understanding of the observed expansion. The northern boundary of *C. gigas*' reproductive niche was unquestionably located south of Bourgneuf Bay (47°N) in the 1970s when *C. gigas* was introduced, and seawater temperature was assumed to be too low for its reproduction further north (Dutertre *et al.*, 2010). This boundary was well represented with our large-scale simulations in cold conditions. Under warmer conditions, this boundary extended up to 60°N, corresponding to a drastic northward shift of more than 1400 km within a few decades; this appears to be consistent with field observations of natural oyster reproduction in British, Belgian, Dutch, Danish, German, Swedish and Norwegian coastal waters, mainly since the 1990s (Wrange *et al.*, 2009; Troost, 2010).

Coastal ecosystems receiving the invasion of *C. gigas* suffer from the consequences related to its ecosystem engineering activities (habitat modification and spatial competition, but also biodiversity enrichment), high filtration rate (carrying capacity, trophic competition) and sediment biodeposition (habitat and food-chain modification) (Padilla, 2010; Troost, 2010; Herbert *et al.*, 2012a). However, these consequences are site-specific and their quantification or prediction is difficult due to the variety of potential effects, as well as the complexity of food-web relationships and interactions. In Bourgneuf Bay, the increase in the wild population of *C. gigas* negatively affected the growth performance of farmed oysters as a

result of trophic and spatial competition, in addition to pressures already exerted by native species such as the mussel *Mytilus edulis*, barnacles and the protected honeycomb worm *Sabellaria alveolata* (Cognie *et al.*, 2006). In addition to environmental issues, there were social and economic consequences to the geographic expansion of *C. gigas*. In France, 60% of oyster farming stocks are currently sustained by natural spat collection. Because spawning conditions became more favourable, Bourgneuf Bay appeared as an emerging spat-collecting sector, with more than 30 oyster farmers developing this activity over the last 5 years. The same tendency was observed to the north, in the Bay of Brest (48.3°N, France) where ten or more oyster farmers now practice spat collection. This has led to important changes in farming practice and the oyster-farming industry at a national scale, and we can expect a profound modification of the geographical distribution of related economic and social activities, in parallel with ecological impacts associated with climate projections (Rombouts *et al*., 2012).

Spatial modelling approaches allow to estimate the fundamental niche of a species and to reveal the areas that this species could potentially colonize (Kearney & Porter, 2009). Due to its spatial coverage and temporal resolution, satellite remote-sensing makes it possible to study the response of marine ecosystems to environmental changes, including phytoplankton decadal variability (Martinez *et al.*, 2009), harmful algal blooms (Stumpf, 2001), eutrophication (Beman *et al.*, 2005), and impact of water quality on shellfish farming (IOCCG, 2009; Thomas *et al.*, 2011; Gernez *et al*., 2014). The combination of ecophysiological modelling with satellite remote sensing therefore allowed us to draw a mechanistic and spatially explicit picture of the reproductive niche of *C. gigas* at a pan-European scale over the last decades.

Importantly, we demonstrated that, besides an overall poleward expansion, the biogeographical distribution of *C. gigas* reproductive niche exhibited complex spatial patterns

associated with mesoscale heterogeneity in seawater temperature (i.e. spawning date did not increase in the cold waters area of the NW of Spain and French Brittany). Micro- and mesoscale heterogeneity in the physical environment may affect the biogeographic responses of intertidal species to climate change (Helmuth *et al.*, 2006b). For example, patterns of aerial body temperature may be more geographically complex due to regional patterns of tidal regime and local wave exposure, and thus create mosaic patterns (Helmuth *et al*., 2006a). Intertidal species can be very sensitive to thermal stress, mainly close to the limits of their expansion range, and extreme temperature variation during aerial exposure may affect their metabolism and survival (Helmuth, 1998). The resolution of the forcing data is therefore an important issue, and the increase of data resolution could reduce potential mismatches between environmental variations and predicted ecological responses (Montalto *et al*., 2014). Due to the advent of a new generation of satellite sensors for coastal zone studies (Vanhellemont *et al.*, 2014), it is expected that remote sensing will become an increasingly valuable tool for biogeography studies. Concurrently, further investigations of fine-scale hydrodynamic and biogeochemical models coupled with individual-based models of larval behaviour could make valuable tools to define the spread of bentho-pelagic species more precisely (Herbert *et al*., 2012b), and thus provide accurate predictions of ecological responses in a changing world.

In conclusion, non-native *C. gigas* showed invasive behaviour on European Atlantic coasts from Gibraltar to Norway. Rise in seawater temperature and coastal phytoplankton enrichment are responsible for this expansion by increasing the fitness potential of *C. gigas*, generally shifting its optimal spawning window and optimal thermal conditions for early life stages poleward. Considering the SST increase projected by the end of the century (IPCC, 2007), coastal ecosystems will be more sensitive to the expansion of non-native species, such as the extension of the Pacific oyster’s geographical range in northern Europe and South

America. In parallel to the ecological implications of such expansion, their social and economic consequences stress the need to broaden our understanding of marine ecosystem responses to global change. This study underlines the importance of studying species' functional traits through individual bioenergetics to understand their response to global change. To this end, the combination of DEB modelling with remote sensing of environmental data is a valuable generic and mechanistic framework that can be used to study the fine- and large-scale biogeographical responses of marine species to global change worldwide.

ACKNOWLEDGEMENTS

This research was funded by the French National Research Agency within the framework of the GIGASSAT project (grants ANR-12-AGRO-0001-01 and ANR-12-AGRO-0001-05). The authors are grateful to the Ifremer staff of the RESCO, VELYGER and REPHY networks, through which all the field data were gathered. We acknowledge S. Petton for his help supplying the satellite data and thank Copernicus/Myocean for providing SST and Ocean Color products. The authors also express their gratitude to H. McCombie for revising the English, and to three anonymous reviewers whose valuable suggestions greatly improved the manuscript.

REFERENCES

Alunno-Bruscia M., Bourlès Y., Maurer D., Robert S., Mazurié J., Gangnery A., Goulletquer P., & Pouvreau S. (2011) A single bio-energetics growth and reproduction model for the oyster *Crassostrea gigas* in six Atlantic ecosystems. *Journal of Sea Research*, **66**, 340–348.

Bacher C. & Gangnery A. (2006) Use of dynamic energy budget and individual based models to simulate the dynamics of cultivated oyster populations. *Journal of Sea Research*, **56**, 140–155.

Beaugrand G., Luczak C., & Edwards M. (2009) Rapid biogeographical plankton shifts in the North Atlantic Ocean. *Global Change Biology*, **15**, 1790–1803.

Beman M.J., Arrigo K.R., & Matson P.A. (2005) Agricultural runoff fuels large phytoplankton blooms in vulnerable areas of the ocean. *Nature*, **434**, 211–214.

Beninger P.G., Valdizan A., Cognie B., Guiheneuf F., & Decottignies P. (2008) Wanted: alive and not dead: functioning diatom status is a quality cue for the suspension-feeder`Crassostrea gigas. *Journal of Plankton Research*, **30**, 689–697.

Bernard I., de Kermoysan G., & Pouvreau S. (2011) Effect of phytoplankton and temperature on the reproduction of the Pacific oyster *Crassostrea gigas*: Investigation through DEB theory. *Journal of Sea Research*, **66**, 349–360.

Bourlès Y., Alunno-Bruscia M., Pouvreau S., Tollu G., Leguay D., Arnaud C., Goulletquer P., & Kooijman S.A.L.M. (2009) Modelling growth and reproduction of the Pacific oyster *Crassostrea gigas*: Advances in the oyster-DEB model through application to a coastal pond. *Journal of Sea Research*, **62**, 62–71.

Briggs J.C. (2007) Marine biogeography and ecology: invasions and introductions. *Journal of Biogeography*, **34**, 193–198.

Carrasco M. & Barón P. (2010) Analysis of the potential geographic range of the Pacific oyster *Crassostrea gigas* (Thunberg, 1793) based on surface seawater temperature satellite data and climate charts: the coast of South America as a study case. *Biological Invasions*, **12**, 2597–2607.

Chavez-Villalba J., Barret J., Mingant C., Cochard J.-C., & Le Pennec M. (2003) Influence of timing of broostock collection on conditioning, oocyte production, and larval rearing of the oyster, *Crassostrea gigas* (Thunberg), at six production sites in France. *Journal of Shellfish Research*, **22**, 465–474.

Cognie B., Haure J., & Barillé L. (2006) Spatial distribution in a temperate coastal ecosystem of the wild stock of the farmed oyster *Crassostrea gigas* (Thunberg). *Aquaculture*, **259**, 249–259.

Dash P., Ignatov A., Martin M., Donlon C., Brasnett B., Reynolds R.W., Banzon V., Beggs H., Cayula J.-F., Chao Y., Grumbine R., Maturi E., Harris A., Mittaz J., Sapper J., Chin T.M., Vazquez-Cuervo J., Armstrong E.M., Gentemann C., Cummings J., Piollé J.-F., Autret E., Roberts-Jones J., Ishizaki S., Høyer J.L., & Poulter D. (2012) Group for High Resolution Sea Surface Temperature (GHRSST) analysis fields inter-comparisons—Part 2: Near real time web-based level 4 SST Quality Monitor (L4-SQUAM). *Satellite Oceanography and Climate Change*, **77–80**, 31–43.

DeAngelis D.L. & Mooij W.M. (2005) Individual-Based Modeling of Ecological and Evolutionary Processes. *Annual Review of Ecology, Evolution, and Systematics*, **36**, 147–168.

Diederich S., Nehls G., van Beusekom J.E.E., & Reise K. (2005) Introduced Pacific oysters (*Crassostrea gigas*) in the northern Wadden Sea: invasion accelerated by warm summers? *Helgoland Marine Research*, **59**, 97–106.

Dutertre M., Beninger P.G., Barillé L., Papin M., & Haure J. (2010) Rising water temperatures, reproduction and recruitment of an invasive oyster, *Crassostrea gigas*, on the French Atlantic coast. *Marine Environmental Research*, **69**, 1–9.

Gernez P., Barillé L., Lerouxel A., Mazeran C., Lucas A., & Doxaran D. (2014) Remote sensing of suspended particulate matter in turbid oyster-farming ecosystems. *Journal of Geophysical Research: Oceans*, **119**, 7277–7294.

Gohin F. (2011) Annual cycles of chlorophyll-a, non-algal suspended particulate matter, and turbidity observed from space and in-situ in coastal waters. *Ocean Science*, **7**, 705–732.

Goulletquer P. & Héral M. (1991) Aquaculture of *Crassostrea gigas* in France. *In* The Ecology of *C. gigas* in Australia, New Zealand, France and Washington State. *Oyster Ecology Workshop, Annapolis, USA*, 12–19.

Helmuth B. (1998) Intertidal mussel microclimates: predicting the body temperature of a sessile invertebrate. *Ecological Monographs*, **68**, 51–74.

Helmuth B., Broitman B.R., Blanchette C.A., Gilman S., Halpin P., Harley C.D.G., O'Donnell M.J., Hofmann G.E., Menge B., & Strickland D. (2006a) Mozaic patterns of thermal stress in the rocky intertidal zone: implications for climate change. *Ecological Monographs*, **76**, 461–479.

Helmuth B., Mieszkowska N., Moore P., & Hawkins S.J. (2006b) Living on the edge of two changing worlds: forecasting the responses of rocky intertidal ecosystems to climate change. *Annual Review of Ecology, Evolution, and Systematics*, **37**, 373–404.

Herbert R.J.H., Roberts C., Humphreys J., & Fletcher S. (2012a) The Pacific oyster (*Crassostrea gigas*) in the UK. Economic, Legal and Environmental issues associated with its cultivation, wild establishment and exploitation. Report to the Shellfish Association of Great Britain. 132 pp.

Herbert R.J.H., Willis J., Jones E., Ross K., Hübner R., Humphreys J., Jensen A., & Baugh J. (2012b) Invasion in tidal zones on complex coastlines: modelling larvae of the non-native Manila clam, *Ruditapes philippinarum*, in the UK. *Journal of Biogeography*, **39**, 585–599.

Hernández-Fariñas T., Soudant D., Barillé L., Belin C., Lefebvre A., & Bacher C. (2013) Temporal changes in the phytoplankton community along the French coast of the eastern English Channel and the southern Bight of the North Sea. *ICES Journal of Marine Science* : *Journal du Conseil*, **71**, 821–833.

Humphreys J., Herbert R.J.H., Roberts C., & Fletcher S. (2014) A reappraisal of the history and economics of the Pacific oyster in Britain. *Aquaculture*, **428–429**, 117–124.

IOCCG (2009) *Remote Sensing in Fisheries and Aquaculture.* (eds Forget, M.-H., Stuart, V. and Platt, T.) Reports of the International Ocean-Colour Coordinating Group, No. 8, IOCCG, Dartmouth, Canada.,

IPCC (2007) *Climate change 2007: impacts, adaptation and vulnerability.* Cambridge, UK: Cambridge University Press.,

Kearney M. & Porter W. (2009) Mechanistic niche modelling: combining physiological and spatial data to predict species' ranges. *Ecology Letters*, **12**, 334–350.

Kearney M., Simpson S.J., Raubenheimer D., & Helmuth B. (2010) Modelling the ecological niche from functional traits. *Philosophical Transactions of the Royal Society B: Biological Sciences*, **365**, 3469–3483.

Kirby R.R. & Beaugrand G. (2009) Trophic amplification of climate warming. *Proceedings of the Royal Society B: Biological Sciences*, **276**, 4095–4103.

Kooijman S.A.L.M. (2006) Pseudo-faeces production in bivalves. *Journal of Sea Research*, **56**, 103–106.

Kooijman S.A.L.M. (2010) *Dynamic Energy Budget Theory for Metabolic Organisation.* Cambridge University Press, Cambridge.

Kristiansen T., Stock C., Drinkwater K.F., & Curchitser E.N. (2014) Mechanistic insights into the effects of climate change on larval cod. *Global Change Biology*, **20**, 1559–1584.

Lejart M. & Hily C. (2011) Differential response of benthic macrofauna to the formation of novel oyster reefs (*Crassostrea gigas*, Thunberg) on soft and rocky substrate in the intertidal of the Bay of Brest, France. *Journal of Sea Research*, **65**, 84–93.

Martinez E., Antoine D., D'Ortenzio F., & Gentili B. (2009) Climate-Driven Basin-Scale Decadal Oscillations of Oceanic Phytoplankton. *Science*, **326**, 1253–1256.

Montalto V., Sarà G., Ruti P.M., Dell'Aquila A., & Helmuth B. (2014) Testing the effects of temporal data resolution on predictions of the effects of climate change on bivalves. *Ecological Modelling*, **278**, 1–8.

O'Connor M.I., Bruno J.F., Gaines S.D., Halpern B.S., Lester S.E., Kinlan B.P., & Weiss J.M. (2007) Temperature control of larval dispersal and the implications for marine ecology, evolution, and conservation. *Proceedings of the National Academy of Sciences*, **104**, 1266–1271.

Padilla D.K. (2010) Context-dependent Impacts of a Non-native Ecosystem Engineer, the Pacific Oyster *Crassostrea gigas*. *Integrative and Comparative Biology*, **50**, 213–225.

Picoche C., Le Gendre R., Flye-Sainte-Marie J., Françoise S., Maheux F., Simon B., & Gangnery A. (2014) Towards the Determination of Mytilus edulis Food Preferences Using the Dynamic Energy Budget (DEB) Theory. *PLoS ONE*, **9**, e109796.

Pörtner H.O., Berdal B., Blust R., Brix O., Colosimo A., De Wachter B., Giuliani A., Johansen T., Fischer T., Knust R., Lannig G., Naevdal G., Nedenes A., Nyhammer G., Sartoris F.., Serendero I., Sirabella P., Thorkildsen S., & Zakhartsev M. (2001) Climate induced temperature effects on growth performance, fecundity and recruitment in marine fish: developing a hypothesis for cause and effect relationships in Atlantic cod (*Gadus morhua*) and common eelpout (*Zoarces viviparus*). *Continental Shelf Research*, **21**, 1975–1997.

Pouvreau S., Bourlès Y., Lefebvre S., Gangnery A., & Alunno-Bruscia M. (2006) Application of a dynamic energy budget model to the Pacific oyster, *Crassostrea gigas*, reared under various environmental conditions. *Journal of Sea Research*, **56**, 156–167.

R Development Core Team (2012) R: A language and environment for statistical computing. *R Foundation for Statistical Computing, Vienna, Austria. http://www.R-project.org/*, .

Rombouts I., Beaugrand G., & Dauvin J.-C. (2012) Potential changes in benthic macrofaunal distributions from the English Channel simulated under climate change scenarios. *Estuarine, Coastal and Shelf Science*, **99**, 153–161.

Sarà G., Palmeri V., Rinaldi A., Montalto V., & Helmuth B. (2013) Predicting biological invasions in marine habitats through eco-physiological mechanistic models: a case study with the bivalve *Brachidontes pharaonis*. *Diversity and Distributions*, **19**, 1235–1247.

Saulquin B. & Gohin F. (2010) Mean seasonal cycle and evolution of the sea surface temperature from satellite and in situ data in the English Channel for the period 1986–2006. *International Journal of Remote Sensing*, **31**, 4069–4093.

Saulquin B., Gohin F., & Garrello R. (2011) Regional Objective Analysis for Merging High-Resolution MERIS, MODIS/Aqua, and SeaWiFS Chlorophyll-a Data From 1998 to 2008 on the European Atlantic Shelf. *Geoscience and Remote Sensing, IEEE Transactions on*, **49**, 143–154.

Saupe E.E., Hendricks J.R., Townsend Peterson A., & Lieberman B.S. (2014) Climate change and marine molluscs of the western North Atlantic: future prospects and perils. *Journal of Biogeography*, **41**, 1352–1366.

Schmidt A., Wehrmann A., & Dittmann S. (2008) Population dynamics of the invasive Pacific oyster *Crassostrea gigas* during the early stages of an outbreak in the Wadden Sea (Germany). *Helgoland Marine Research*, **62**, 367–376.

Stachowicz J.J., Terwin J.R., Whitlatch R.B., & Osman R.W. (2002) Linking climate change and biological invasions: Ocean warming facilitates nonindigenous species invasions. *Proceedings of the National Academy of Sciences*, **99**, 15497–15500.

Stumpf R.P. (2001) Applications of Satellite Ocean Color Sensors for Monitoring and Predicting Harmful Algal Blooms. *Human and Ecological Risk Assessment: An International Journal*, **7**, 1363–1368.

Tamayo D., Ibarrola I., Urrutxurtu I., & Navarro E. (2014) Physiological basis of extreme growth rate differences in the spat of oyster (*Crassostrea gigas*). *Marine Biology*, **161**, 1627–1637.

Taylor K.E. (2001) Summarizing multiple aspects of model performance in a single diagram. *Journal of Geophysical Research: Atmospheres*, **106**, 7183–7192.

Teal L.R., van Hal R., van Kooten T., Ruardij P., & Rijnsdorp A.D. (2012) Bio-energetics underpins the spatial response of North Sea plaice (*Pleuronectes platessa* L.) and sole (*Solea solea* L.) to climate change. *Global Change Biology*, **18**, 3291–3305.

Thomas Y., Mazurié J., Alunno-Bruscia M., Bacher C., Bouget J.-F., Gohin F., Pouvreau S., & Struski C. (2011) Modelling spatio-temporal variability of *Mytilus edulis* (L.) growth by forcing a dynamic energy budget model with satellite-derived environmental data. *Journal of Sea Research*, **66**, 308–317.

Troost K. (2010) Causes and effects of a highly successful marine invasion: Case-study of the introduced Pacific oyster *Crassostrea gigas* in continental NW European estuaries. *Journal of Sea Research*, **64**, 145–165.

Van der Meer J. (2006) Metabolic theories in ecology. *Trends in Ecology and Evolution*, **21**, 136–140.

Vanhellemont Q., Neukermans G., & Ruddick K. (2014) Synergy between polar-orbiting and geostationary sensors: Remote sensing of the ocean at high spatial and high temporal resolution. *Liege Colloquium Special Issue: Remote sensing of ocean colour, temperature and salinity*, **146**, 49–62.

Wrange A.L., Valero J., Harkestad L.S., Strand Ø., Lindegarth S., Christensen H.T., Dolmer P., Kristensen P.S., & Mortensen S. (2009) Massive settlements of the Pacific oyster, *Crassostrea gigas*, in Scandinavia. *Biological Invasions*, **12**, 1453–1458.

SUPPORTING INFORMATION

Additional Supporting Information may be found in the online version of this article:

Appendix S1 Supplementary details on the oyster-DEB model design and initialization.

Appendix S2 Supplementary details on the forcing variables used for the DEB model simulations.

BIOSKETCH

Y. Thomas is currently a post-doctoral researcher at the University of Nantes (France), studying the response of shellfish ecosystems to environmental change, using historical and experimental data, and modelling approaches.

Author contributions: All authors designed the study; Y.T., P.G. and S.P. provided environmental and oyster data; F.G. and P.B. provided the satellite data; Y.T. ran the model and analysed the results; Y.T. and P.G. wrote the paper. All authors discussed the results and commented on and improved the manuscript.

Editor: Daniel Chapman

Table 1. ANOVA performed on summer sea surface temperature (SST) and spawning date (in Julian days) predicted to test the difference between times (2 periods: 1960 to 1987 *versus* 1988 to 2013), food scenarios (low, mean, high), and their interaction.

		d.f.	MS	*F*	*P*
SST	Time	1	2.0	6.69	*
	Residuals	52	0.3		
Spawning date	Time	1	2482.9	15.49	***
	Food	2	3.6	0.02	n.s.
	Time × Food	2	7.9	0.05	n.s.
	Residuals	156	160.3		

n.s. = not significant
* $P < 0.05$; *** $P < 0.001$

FIGURES

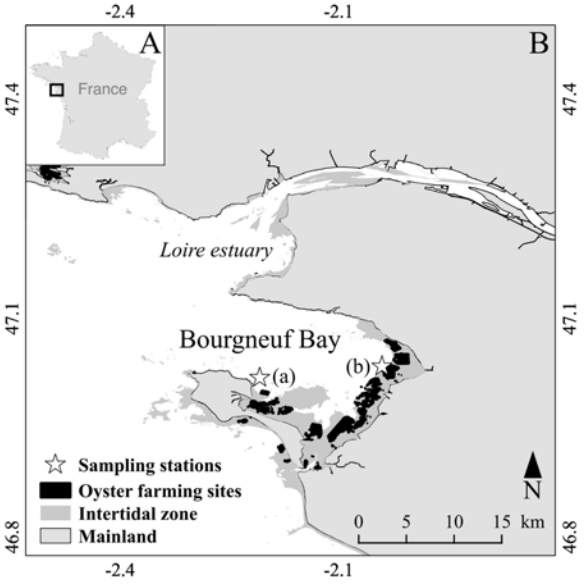

Fig. 1. Location of Bourgneuf Bay on the French Atlantic coast (A); bay morphology (B). Locations of the oyster farming sites and sampling stations (stars): (a) “Bois de la Chaise” and (b) “La Coupelasse”.

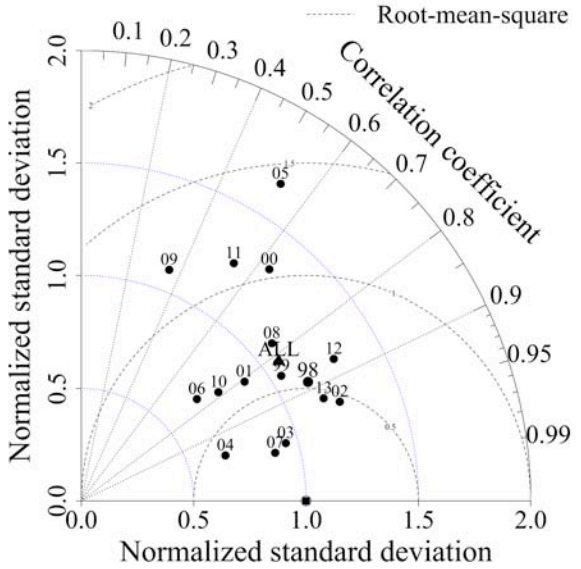

Fig. 2. Taylor diagram giving the correlation, root-mean-square (RMS) difference and the ratio of variances between predicted and observed values of individual dry flesh mass (DFM). Numbers on the plot give the evaluation for each year from 1998 to 2013, and “All” represents the overall model evaluation.

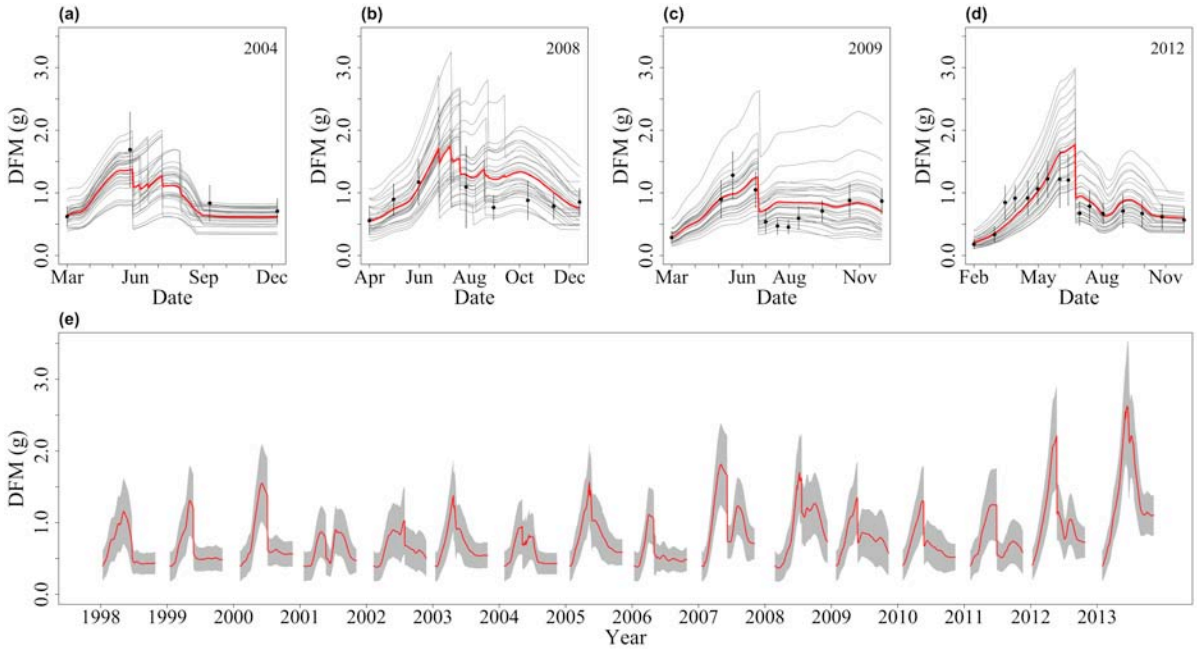

Fig. 3. Simulations of the oyster dry flesh mass (DFM): (a-d) validation step, with 4 examples of observed (black points ± standard deviation) *versus* simulated DFM (30 individual trajectories, in grey, with averages of all individuals shown by bold lines), for 2004, 2008, 2009 and 2012 (Figure S2 gives all years). (e) Application step, with standard initial state for all yearly simulations, from 1998 to 2013 (averages of all individuals shown by bold lines ± standard deviation in grey shading).

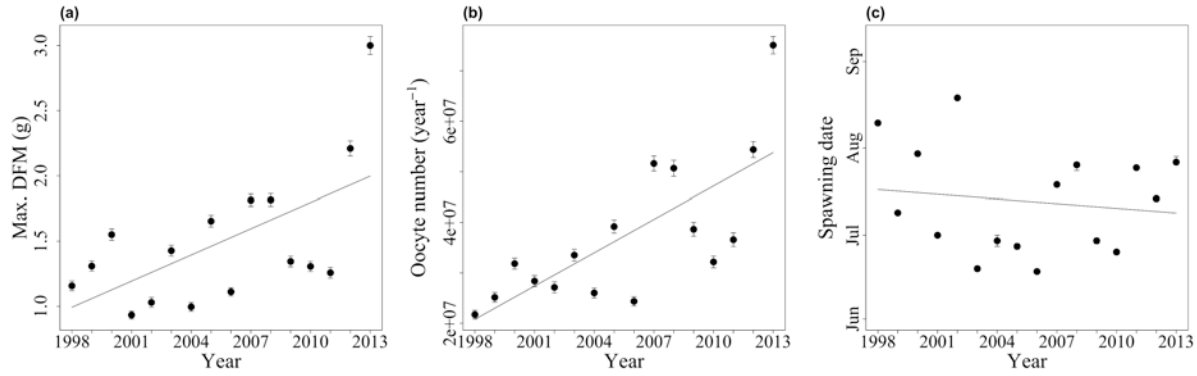

Fig. 4. Yearly simulated life-history traits with the ± 95% confidence interval: (a) maximum dry flesh mass (Max. DFM), (b) oocyte number produced, and (c) spawning date. The lines represent the linear regression.

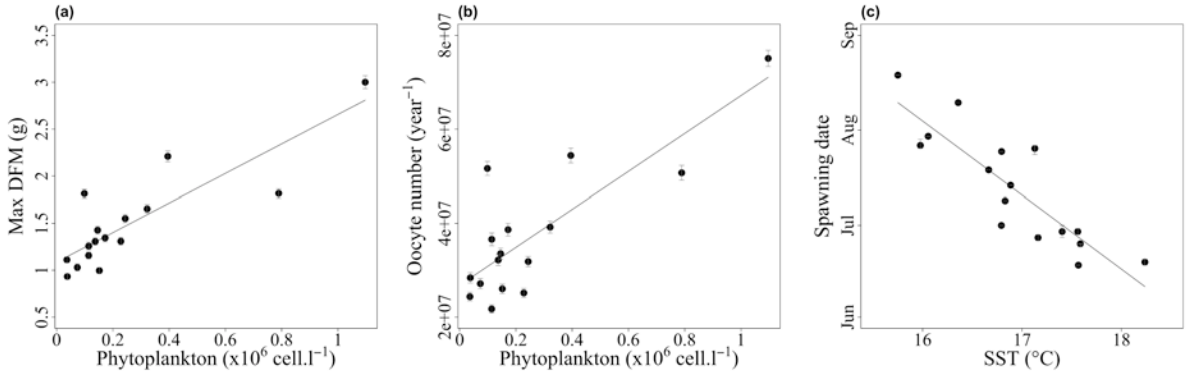

Fig. 5. Correlation between the late-spring forcing average (1st June to 15 July) and oyster life history traits: (a) maximum dry flesh mass (Max DFM) *versus* late-spring phytoplankton concentration average, (b) oocyte production *versus* late-spring phytoplankton concentration average, and (c) spawning date *versus* late-spring sea surface temperature (SST) average. The data represent the averages of individual ± 95% confidence interval.

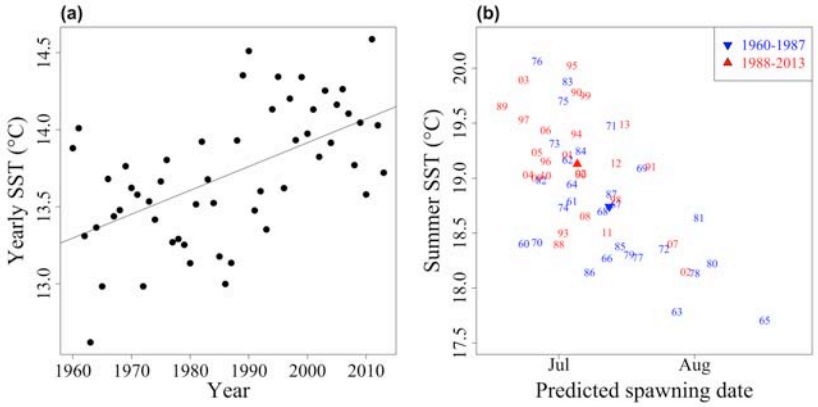

Fig. 6. Effect of global warming on the Bourgneuf Bay ecosystem since 1960: (a) time series of yearly sea surface temperature (SST), (b) summer SST plotted on simulated spawning date. Since no difference was measured between food and PIM scenarios (see Table 1), only the "mean" scenario is presented.

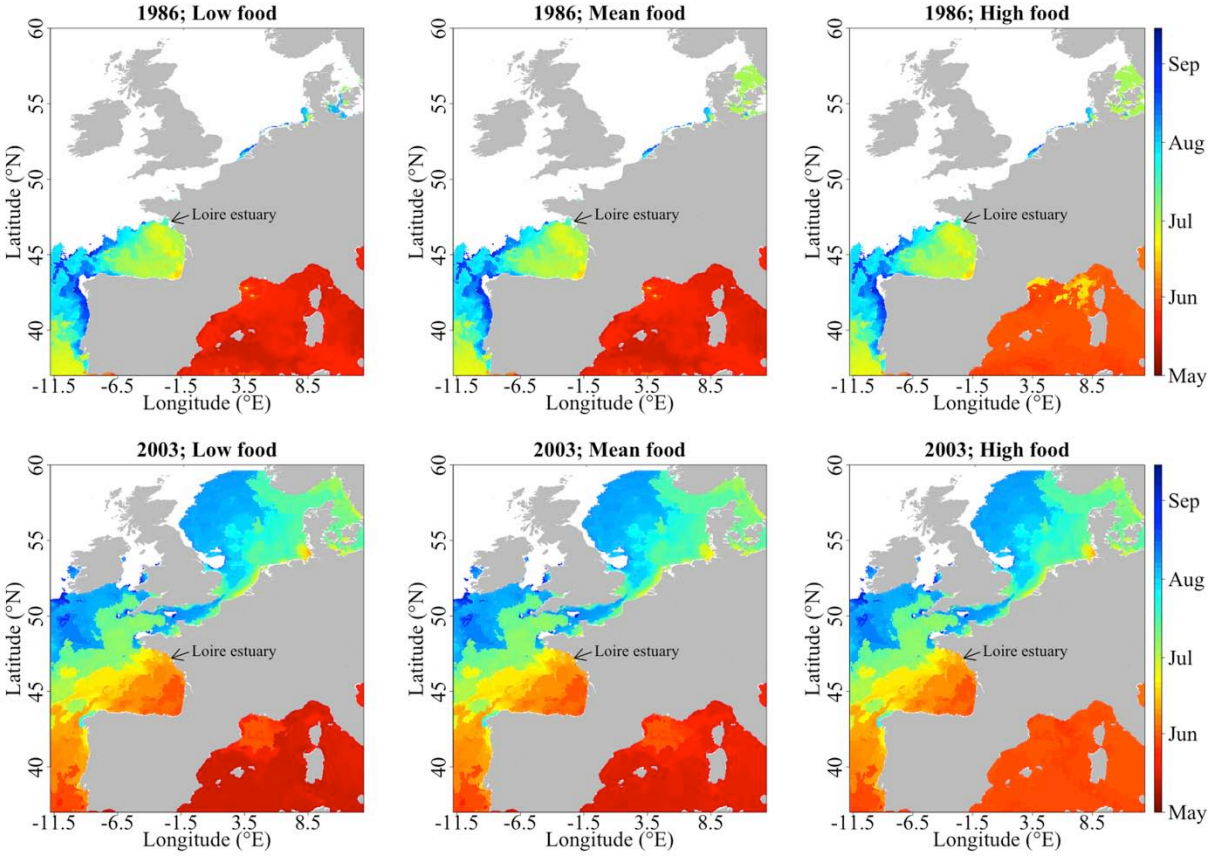

Fig. 7. Simulated spatial distribution of Pacific oyster spawning date along the European coasts for two contrasted years: cold scenario in 1986 and warm scenario in 2003, and the three investigated food and PIM scenarios: low, mean and high. No spawns occurred in the areas coloured white.

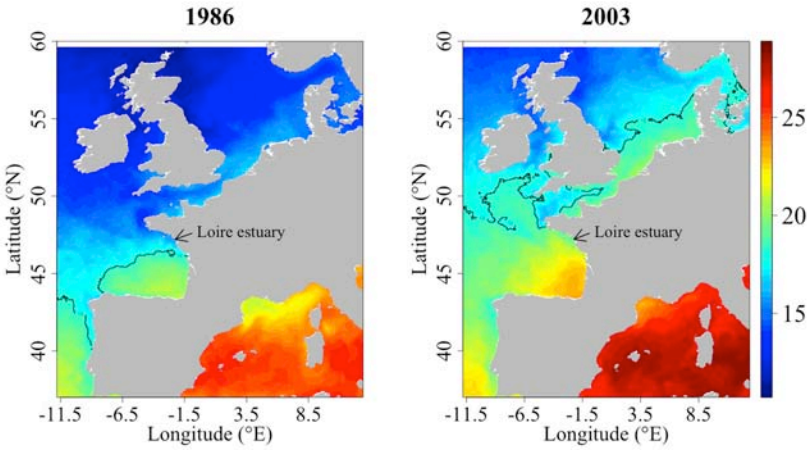

Fig. 8. Mean summer sea surface temperature (SST) averaged from 15 July to 15 September: (a) cold scenario in 1986 and (b) warm scenario in 2003. Contour lines represent the mean summer isotherm of 18°C.

Journal of Biogeography

SUPPORTING INFORMATION

Global change and climate-driven invasion of the Pacific oyster (*Crassostrea gigas*) along European coasts: a bioenergetics modelling approach

Yoann Thomas, Stéphane Pouvreau, Marianne Alunno-Bruscia, Laurent Barillé, Francis Gohin, Philippe Bryère, Pierre Gernez

Appendix S1 Supplementary details on the oyster-DEB model design and initialization, and additional figures (Figures S1 - S2) and tables (Tables S1 – S2).

The oyster-DEB model

The DEB model used in the present study to simulate oyster growth and reproduction was derived from the standard DEB model described by Kooijman (2010) and first applied to *C. gigas* by Pouvreau *et al.* (2006). The model equations and parameter values used here are based mainly on the study by Bernard *et al.* (2011), which refined the processes of energy allocation to gametogenesis and resorption. The conceptual scheme of the model is described in Figure S1Figure S1. The flux equations and parameters are summarized in Table S1 and S2, respectively.

Briefly, the DEB model describes the dynamics of four state variables: the energy stored in reserves, E; the energy allocated to structural volume growth, V; the energy allocated to development and reproduction, E_R; and the energy used in gamete construction, E_{GO}. A

constant fraction, κ, of reserve mobilization rate, $\dot{p}_{C1}$, is allocated from reserves for structural growth and maintenance; whereas the remainder, (1-κ), is allocated to development/reproduction and maturity maintenance. Gonad construction is modelled similarly to structural building, through the gamete mobilization rate, $\dot{p}_{C2}$. Therefore, the number of oocytes may be estimated by dividing E_{G0} by the energy content of one oocyte. All metabolic rates are controlled by temperature, according to the Arrhenius function (Eq. 1).

In case of starvation, maintenance costs are prioritized over growth and reproduction. The gametogenesis flux is then allocated for maintenance costs through the emergency maintenance rate, $\dot{p}_{M2}$. If $\dot{p}_{M2}$ does not cover all maintenance costs, the gamete resorption rate, $\dot{p}_{L2}$, takes over. In case of extreme starvation, the structure is broken down at the rate $\dot{p}_{L1}$.

In the oyster-DEB model, spawning is triggered when two thresholds are reached: a temperature threshold set at 18°C (Cognie *et al.*, 2006; Dutertre *et al.*, 2010), and a gameto-somatic index (GSI) threshold of 40%, where GSI is defined as a mass ratio between the gonadic and total dry flesh mass (Pouvreau *et al.*, 2006).

As *C. gigas* is an intertidal species, an immersion factor, T_{im}, was applied to the ingestion function to take into account the influence of tidal emersion on oyster growth (see Eq. 2, Table S1). T_{im} was computed as the average daily percentage time during which oysters are immerged, using 16 years of hourly sea level data, and considering that oysters were fixed at a height of 2 m above zero tide level.

Model initialization

The initialization of the state variables for the simulated individuals was performed according to their initial individual length (L) and dry flesh mass (DFM), which were extracted from REMORA/RESCO data.

The values of the DEB parameters used in the present study are summarized in Table S2. *C. gigas* gametogenesis is known to start in early spring, when temperature rises above 10–11°C (Ruiz *et al.*, 1992). Simulations were started on the first of March, with temperature lower than this threshold; the gamete compartment, E_{GO}, was considered empty at the initial state. The initial structural volume, V, was estimated according to the length measurement (L), and the shape coefficient (δ), considering the relationship $V = (L.\delta)^3$. The initial energy stored in the reserve compartment, E, was calculated according to the formula $E = e.[Em].V$, where e is the scaled energy density, and [Em] the maximum reserve density. The scaled energy density (e = [E]/[Em]) tends to approach the value of the scaled functional response (Pouvreau *et al.*, 2006). Initial scaled energy density was consequently considered low, at e = 0.1, considering the low trophic and thermal conditions in winter. Finally, the initial energy stored in the development/reproduction buffer, E_R, was deducted from the total amount of initial energy calculated from the DFM and from the amount of energy stored in E and V, following equation 16 in Table S1.

Supplementary tables (Tables S1 – S2)

Table S1. Equations describing the energy fluxes and state variable differential equations in the Dynamic Energy Budget (DEB) model. X corresponds to the phytoplankton concentration, T to the water temperature (K) and Y to the suspended particulate inorganic matter concentration (PIM).

N°	Description	Equation
(1)	Temperature effect	$c_T = exp\left\{\frac{T_A}{T_{ref}} - \frac{T_A}{T}\right\} \cdot \left(1 + exp\left\{\frac{T_{AL}}{T_{ref}} - \frac{T_{AL}}{T_L}\right\} + exp\left\{\frac{T_{AH}}{T_H} - \frac{T_{AH}}{T_{ref}}\right\}\right) \cdot \left(1 + exp\left\{\frac{T_{AL}}{T} - \frac{T_{AL}}{T_L}\right\} + exp\left\{\frac{T_{AH}}{T_H} - \frac{T_{AH}}{T}\right\}\right)^{-1}$
(2)	Ingestion rate	$\dot{p}_X = \{\dot{j}_{Xm}\} \cdot f \cdot V^{2/3} \cdot c_T \cdot T_{im}$
(2')	Functional response	$f = \frac{X}{X + K(Y)}$
(2'')	Half saturation coefficient	$K(Y) = Xk(1 + \frac{Y}{Xk_Y})$
(3)	Assimilation rate	$\dot{p}_A = \kappa_X \cdot \dot{p}_X$
(4)	Reserve mobilization rate	$\dot{p}_{C1} = [E]\frac{c_T[E_G]\dot{v}V^{2/3} + c_T[\dot{p}_M]}{\kappa[E] + [E_G]}$ $with\ [E] = E/V$
(5)	Structural maintenance rate	$\dot{p}_{M1} = [\dot{p}_M] \cdot V \cdot c_T$
(6)	Structural growth rate	$\dot{p}_G = \kappa \cdot \dot{p}_{C1} - \dot{p}_{M1}$
(7)	Maturity maintenance rate	$\dot{p}_J = min(V, V_P) \cdot [\dot{p}_M] \cdot \left(\frac{1-\kappa}{\kappa}\right) \cdot c_T$
(8)	Maturation and reproduction rate	$\dot{p}_R = (1-\kappa) \cdot \dot{p}_{C1} - \dot{p}_J$
(10)	Lysis of structure rate	$\dot{p}_{L1} = max(\dot{p}_{M1} - (\kappa\dot{p}_{C1} + \dot{p}_{M2} + \dot{p}_{L2}), 0)$
(11)	Gamete mobilization rate	$\dot{p}_{C2} = E_R\left(\frac{\{\dot{p}_{Am}\} \cdot c_T}{[Em] \cdot V^{1/3}} + \frac{[\dot{p}_M] \cdot c_T}{[E_G]}\right) \cdot \left(1 - \kappa \cdot \frac{E}{[E_G] \cdot V + \kappa \cdot E}\right)$
(12)	Emergency maintenance rate	$\dot{p}_{M2} = min(\dot{p}_{M1} - \kappa\dot{p}_{C1}, \dot{p}_{C2})$
(13)	Gonad allocation rate	$\dot{p}_{Go} = \dot{p}_{C2} - \dot{p}_{M2}$
(14)	Gamete resorption rate	$\dot{p}_{L2} = max\left(\frac{\dot{p}_{M1} - \kappa \cdot \dot{p}_{C1} + \dot{p}_{M2}}{Y_{Go}}, 0\right)$
(16)	Total dry flesh mass calculation	$DFM = \frac{E + E_R}{\rho_E} + V \cdot d_V + \frac{E_{Go} \cdot d_{Go}}{[E_{Ggo}]}$
State variable differential equations		
(17)	Reserves	$\frac{dE}{dt} = \dot{p}_A - \dot{p}_{c1}$
(18)	Structural volume	$\frac{dV}{dt} = \frac{\dot{p}_G - \dot{p}_{L1}}{[E_G]}$
(19)	Development/reproduction	$\frac{dE_R}{dt} = \dot{p}_R - \dot{p}_{c2}$
(20)	Gametes	$\frac{dE_{GO}}{dt} = \dot{p}_{GO} - \dot{p}_{L2} - spawning$

Table S2. Dynamic Energy Budget (DEB) parameters used in the present study

Parameter description	Symbol	Value	Unit
Main parameters			
Shape coefficient	δ_M	0.175	-
Maximum surface specific ingestion rate	$\{\dot{p}_{Xm}\}$	1027	J cm^{-2} d^{-1}
Volume specific maintenance cost	$[\dot{p}_M]$	44	J cm^{-3} d^{-1}
Volume specific cost for structural growth	$[E_G]$	3900	J cm^{-3}
Maximum reserve density	$[E_m]$	4200	J cm^{-3}
Allocation fraction to growth and maintenance	κ	0.45	-
Assimilation efficiency	κ_X	0.75	-
Reproduction efficiency	κ_R	0.75	-
Food half saturation coefficient	Xk	0.32	10^6 cell L^{-1}
PIM half saturation coefficient	Xk_Y	40	mg L^{-1}
Additional and compound parameters			
Energy content of 1 g of reserve	ρ_E	19600	J g^{-1}
Dry mass ratio of structure	d_V	0.15	g_{dw} g_{ww}^{-1}
Dry mass ratio of gonad	d_{GO}	0.31	g_{dw} g_{ww}^{-1}
Volume specific cost for gonad	$[E_{Ggo}]$	7500	J cm^{-3}
Energy conductance	$\dot{v} = \kappa_X\{\dot{p}_{Xm}\}/[E_m]$	0.183	cm d^{-1}
Yield of gonad tissue used for maintenance	Y_{go}	0.25	-
Volume at puberty	V_p	0.4	cm^3
Percentage of immersion	T_{im}	0.75	-
Temperature effect			
Arrhenius temperature	T_A	5800	K
Reference temperature	T_{ref}	293	K
Lower boundary tolerance range	T_L	281	K
Upper boundary tolerance range	T_H	300	K
Arrhenius temp. for lower boundary	T_{AL}	75000	K
Arrhenius temp. for upper boundary	T_{AH}	30000	K

Supplementary figures (Figures S1 and S2)

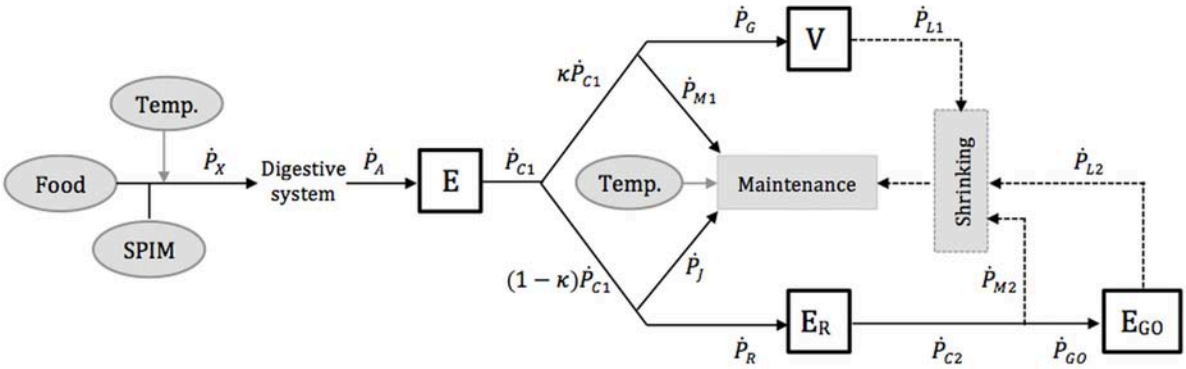

Figure S1 Conceptual scheme of energy fluxes through the Dynamic Energy Budget (DEB) model. State variables (i.e., E, V, E_R, E_{GO}) are represented by squares, and forcing variables by rounded shapes.

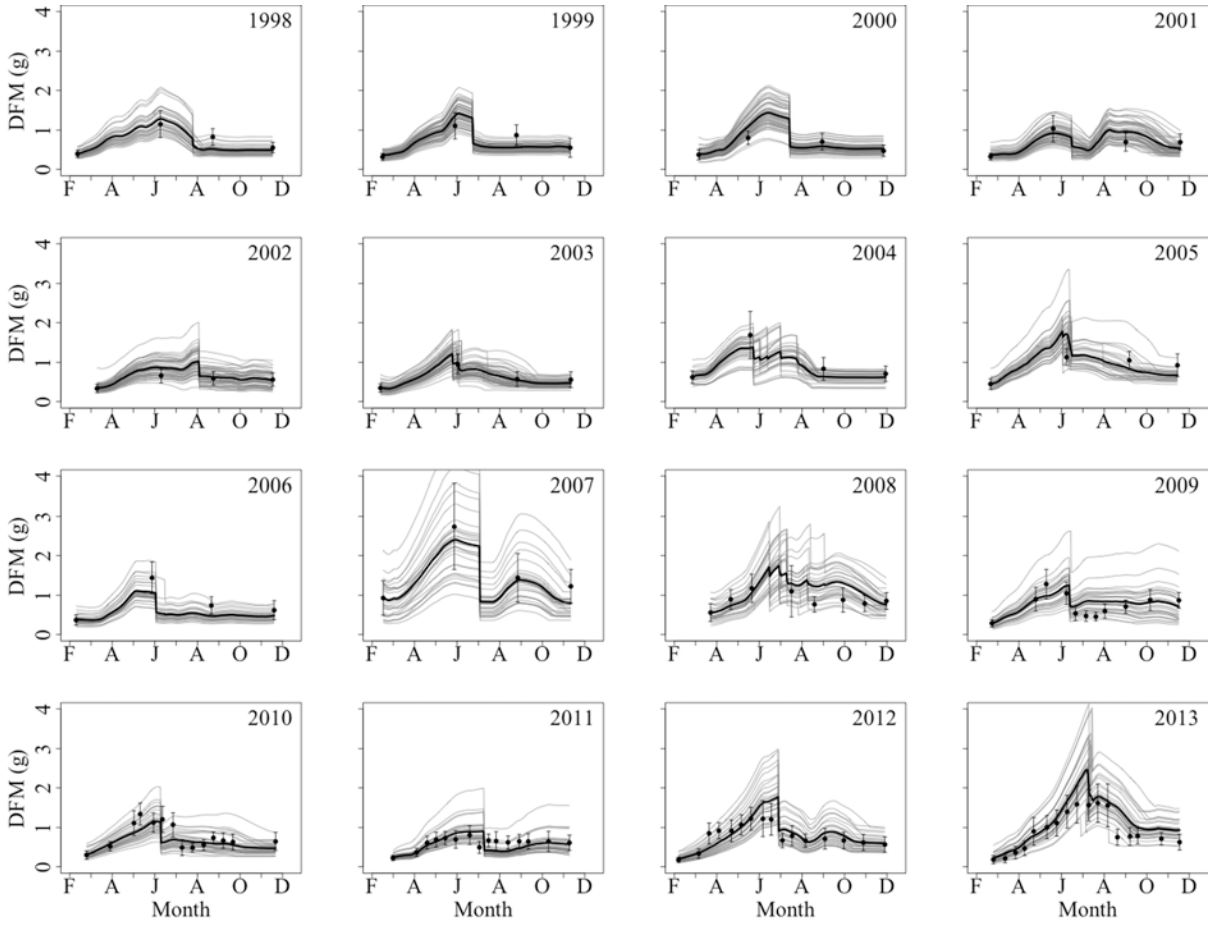

Figure S2 Dry flesh mass (DFM), observed (black points ± standard deviation) and simulated (30 individual trajectories in grey with averages of all individuals shown by bold lines), from 1998 to 2013.

REFERENCES

Bernard I., de Kermoysan G., & Pouvreau S. (2011) Effect of phytoplankton and temperature on the reproduction of the Pacific oyster *Crassostrea gigas*: Investigation through DEB theory. *Journal of Sea Research*, 66, 349–360.

Cognie B., Haure J., & Barillé L. (2006) Spatial distribution in a temperate coastal ecosystem of the wild stock of the farmed oyster *Crassostrea gigas* (Thunberg). *Aquaculture*, 259, 249–259.

Dutertre M., Beninger P.G., Barillé L., Papin M., & Haure J. (2010) Rising water temperatures, reproduction and recruitment of an invasive oyster, *Crassostrea gigas*, on the French Atlantic coast. *Marine Environmental Research*, 69, 1–9.

Kooijman S.A.L.M. (2010) *Dynamic Energy Budget Theory for Metabolic Organisation.* Cambridge University Press, Cambridge.

Pouvreau S., Bourlès Y., Lefebvre S., Gangnery A., & Alunno-Bruscia M. (2006) Application of a dynamic energy budget model to the Pacific oyster, *Crassostrea gigas*, reared under various environmental conditions. *Journal of Sea Research*, 56, 156–167.

Ruiz C., Abad M., Sedano F., Garcia-Martin L.O., & López J.L.S. (1992) Influence of seasonal environmental changes on the gamete production and biochemical composition of *Crassostrea gigas* (Thunberg) in suspended culture in El Grove, Galicia, Spain. *Journal of Experimental Marine Biology and Ecology*, 155, 249–262.

Journal of Biogeography

SUPPORTING INFORMATION

Global change and climate-driven invasion of the Pacific oyster (*Crassostrea gigas*) along European coasts: a bioenergetics modelling approach

Yoann Thomas, Stéphane Pouvreau, Marianne Alunno-Bruscia, Laurent Barillé, Francis Gohin, Philippe Bryère, Pierre Gernez

Appendix S2 Supplementary details on the forcing variables used for the DEB model simulations and result analysis.

Forcing variables for DEB model calibration/application

The mean sea surface temperature (SST) measured by satellite remote sensing was 13.8°C in Bourgneuf Bay over the last 16 years. SST varied seasonally, with an average minimum of 8.8 ± 0.8°C in February and an average maximum of 19.1 ± 1.3°C in August (Fig S3a). Daily extremes reached 6.8 °C in February 2010 and 22.7°C in August 2003. The maximum annual average (14.4 ± 0.2°C) occurred in 2003, and the minimum annual average (13.0 ± 0.2°C) was observed in 2010 (Fig S3b). Late-spring averaged SST, computed as the mean SST from 1 June to 15 July, was 16.9 ± 0.7°C over the last 16 years, ranging from extremes of 15.8 ± 0.03°C in 2002 to 18.2 ± 0.05°C in 2003.

Annual phytoplankton concentration averaged 0.21 ± 0.17 × 10^6 cell L^{-1} (Fig S3c). Averaged phytoplankton concentration exhibited a seasonal pattern, with a maximum in

April: 0.87 ± 1.11 × 10^6 cell L^{-1}, and a minimum in December: 0.02 ± 0.01 × 10^6 cell L^{-1}. The annual spring bloom started in March and finished at the end of July. The maximum yearly average was observed in 2013, at 0.79 ± 0.07 × 10^6 cell L^{-1}, and the minimum in 2004, at 0.10 ± 0.01 × 10^6 cell L^{-1}, with an overall increase during the 1998–2013 period (Fig S3d). Late-spring phytoplankton concentration averaged 0.26 ± 0.29 × 10^6 cell L^{-1} over the 16-year period, with a maximum in 2013: 1.10 ± 0.02 × 10^6 cell L^{-1}, and minimum in 2006: 0.04 ± 0.00 × 10^6 cell L^{-1}. Late-spring phytoplankton concentration was generally similar to the annual mean, with the exception of 2008, which had a late-spring concentration (0.79 ± 0.01 × 10^6 cell L^{-1}) significantly higher than the annual mean (0.18 ± 0.01 × 10^6 cell L^{-1}).

Particulate inorganic matter (PIM) concentration varied seasonally, with a winter maximum of 103 ± 147 mg L^{-1} and summer minimum of 7 ± 4 mg L^{-1} (Fig S3e). Yearly average was 28 ± 48 mg L^{-1}. Maximum yearly average was observed in 2007: 50 ± 6 mg L^{-1}, and minimum in 2004: 15 ± 1 mg L^{-1} (Fig S3f). The mean late-spring PIM concentration (10 ± 3 mg L^{-1}) was lower than the annual mean. The maximum late-spring PIM concentration was observed in 1998 (15 ± 1 mg L^{-1}) and the minimum in 2003 (7 ± 0.1 mg L^{-1}).

Large-scale retrospective food and SST scenarios

To test the sensitivity of the model predictions to variations in phytoplankton and PIM concentration, three realistic scenarios were tested: low, mean and high food-PIM levels. A hierarchical analysis, based on a distance matrix, computed on daily food-PIM profiles, allowed us to select the most contrasted years: 2004 for the low level and 2007 for the high level (Fig. S4a–b). For the mean level, a daily average was calculated, based on the

16-year data set. Three daily profiles were thus extracted and used for the large-scale historical simulations.

At the European scale, two contrasted thermal conditions were selected. SST data were spatially averaged at a daily resolution (Fig. S4c). The most contrasted years: cold-1986 (yearly average SST computed on the overall European scale of 12.99°C) and warm-2003 (yearly average of 14.25°C) (ANOVA, d.f. = 1, $F = 18.9$, $P < 0.001$) were selected and used to explore the consequences for oyster life history traits.

Supplementary figures (Figures S3 and S4)

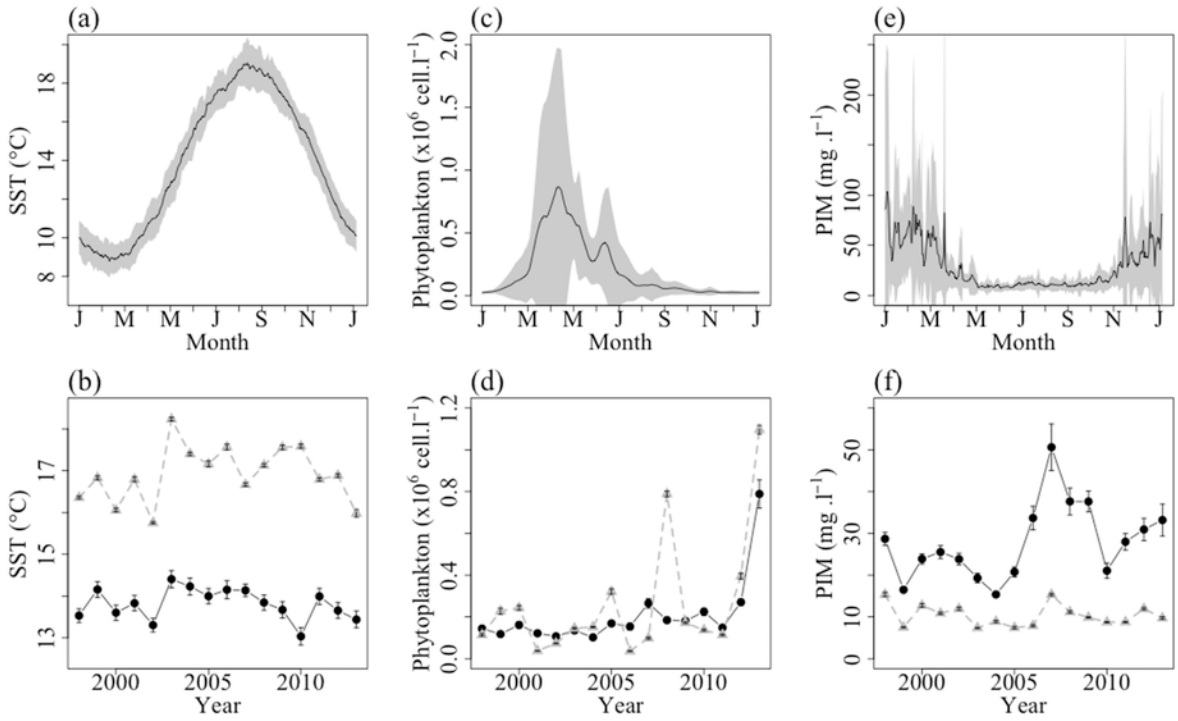

Figure S3 Averaged daily time series of the three forcing variables: (a) sea surface temperature (SST), (c) phytoplankton concentration and (e) particulate inorganic matter (PIM) concentration, obtained from 16 years of observation (grey area represents the standard deviation envelope); annual averages ± standard error (black circles, plain line) and annual late-spring (1st June to 15th July) averages ± standard error (grey triangles, dotted line) of (b) SST, (d) phytoplankton concentration and (f) PIM concentration, from 1998 to 2013

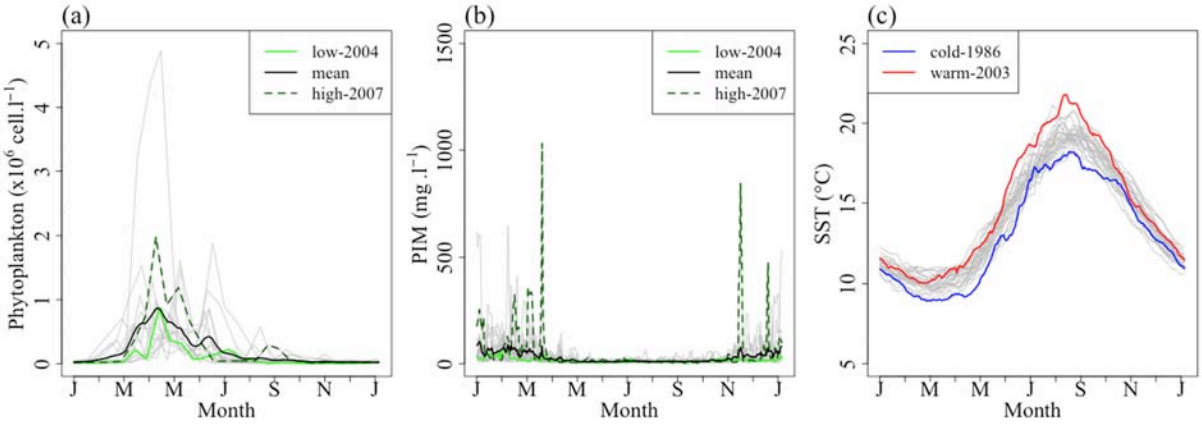

Figure S4 Daily time series of: (a) phytoplankton concentration and (b) particulate inorganic matter (PIM) concentration for the three feeding scenarios: low, mean and high food-PIM levels (the other years are in grey) and (c) sea surface temperature (SST, °C), for the two SST conditions: cold and warm (the other years are shown in grey).

REFERENCES

Bernard I., de Kermoysan G., & Pouvreau S. (2011) Effect of phytoplankton and temperature on the reproduction of the Pacific oyster *Crassostrea gigas*: Investigation through DEB theory. *Journal of Sea Research*, 66, 349–360.

Cognie B., Haure J., & Barillé L. (2006) Spatial distribution in a temperate coastal ecosystem of the wild stock of the farmed oyster *Crassostrea gigas* (Thunberg). *Aquaculture*, 259, 249–259.

Dutertre M., Beninger P.G., Barillé L., Papin M., & Haure J. (2010) Rising water temperatures, reproduction and recruitment of an invasive oyster, *Crassostrea gigas*, on the French Atlantic coast. *Marine Environmental Research*, 69, 1–9.

Kooijman S.A.L.M. (2010) *Dynamic Energy Budget Theory for Metabolic Organisation.* Cambridge University Press, Cambridge.

Pouvreau S., Bourlès Y., Lefebvre S., Gangnery A., & Alunno-Bruscia M. (2006) Application of a dynamic energy budget model to the Pacific oyster, *Crassostrea gigas*, reared under various environmental conditions. *Journal of Sea Research*, 56, 156–167.

Ruiz C., Abad M., Sedano F., Garcia-Martin L.O., & López J.L.S. (1992) Influence of seasonal environmental changes on the gamete production and biochemical composition of *Crassostrea gigas* (Thunberg) in suspended culture in El Grove, Galicia, Spain. *Journal of Experimental Marine Biology and Ecology*, 155, 249–262.